Abstract E-106 Table 3 Technical nuances and steps for telescoping pipelines

ACCESS and SUPPORT	The pipeline wire needs to be advanced distally and the intermediate catheter advanced distally prior to tracking the microcatheter through the pipeline to ensure access. Often times the intermediate catheter will be advanced to the pipeline or even into the first pipeline for proper access.
SIZING (diameter)	The second pipeline needs to be of the same or larger diameter than the first one to prevent an endoleak due to a too small second pipeline diameter.
SIZING (length)	The second pipeline needs to overlap about 50% with the first one for the final telescoping construct. The large overlap percentage bears the risk of a shorter construct (in length) than anticipated.
PIPELINE APPOSITION	Mal-apposition of the telescoping pipelines will result in an endoleak and in a potentially catastrophic thrombotic complication. Gentle angioplasty is important to ascertain perfect apposition of the telescoping construct. In instances where angioplasty has a higher risk (ruptured blister aneurysms, iatrogenic pseudoaneurysms) the construct can be massaged with an 18 microwire in its entire diameter to expand the pipelines into a well apposed construct.

patients, 15%). Distribution of telescoping type was as follows: 21 aneurysms (44%) were treated with proximal extension, 13 aneurysms (27%) with distal extension and 14 aneurysms (29%) with FD placement inside one another. Thirty patients (70%) had complete aneurysm occlusion at follow-up. Two patients (4%) had to be retreated. Four patients (9%) had a permanent intraprocedural complication.

Conclusion We present a multi-institutional case series that focuses on the technical nuances and challenges of telescoping pipelines for the treatment of intracranial aneurysms. These data indicate a higher-than-expected complication rate that is likely due to the technical complexity of these cases. We hope these cases further educates the reader on the indications and challenging aspects of telescoping pipeline devices.

Disclosures C. Baker: None. **J. Hunsaker:** None. **Z. Folzenlogen:** None. **D. Case:** None. **G. Pride:** None. **J. White:** None. **C. Roark:** None. **B. Welch:** None. **A. White:** None. **J. Seinfeld:** None. **R. Grandhi:** None. **P. Taussky:** None.

E-107 MULTI-CENTER STUDY OF A DEEP LEARNING MODEL FOR INTRACRANIAL ANEURYSM DETECTION IN COMPUTED TOMOGRAPHY ANGIOGRAPHY

[1,2]D Wu, [3]E Orru', [4]S Ferraciolli, [5,6]A Ashok, [7,8]A Sorby-Adams, [9]M Guindy, [10,2]D Montes, [11]A Medina, [4]G Bianco, [5,6]J Kaggie, [9]D Rabina, [12]O Ashush, [12]X Han, [12]Y Baror, [12]M Patel, [12]I Dayan, [10,2]J Romero, [10,2]R González, [11]C Wald, [4]F Kitamura, [4]P Kuriki, [5,6]T Matys, [1,2]Q Li. *[1]Center for Advanced Medical Computing and Analysis, Massachusetts General Hospital, Boston, MA; [2]Harvard Medical School, Boston, MA; [3]Department of Interventional Neuroradiology, Lahey Hospital and Medical Center, Burlington, MA; [4]Dasalnova, Diagnósticos da América SA (DASA), São Paulo, BRAZIL; [5]Department of Radiology, Addenbrooke's Hospital, Cambridge University Hospital NHS Foundation Trust, Cambridge, UK; [6]Department of Radiology, University of Cambridge, Cambridge, UK; [7]MRC Mitochondrial Biology Unit, University of Cambridge, Cambridge, UK; [8]Department of Medicine, University of Cambridge, Cambridge, UK; [9]Department of Imaging, Assuta Medical Center, Tel Aviv-Yafo, ISRAEL; [10]Department of Radiology, Massachusetts General Hospital, Boston, MA; [11]Department of Radiology, Lahey Hospital and Medical Center, Burlington, MA; [12]Rhino HealthTech Inc., Boston, MA*

10.1136/neurintsurg-2022-SNIS.218

Introduction CT angiography (CTA), the modality of choice for detection of intracranial aneurysms (IA), is widely available at all care levels. Implementing deep learning algorithms (DLA) in the radiologists' workflow could result in higher detection rates, particularly in smaller centers. We present results of multicenter pre-clinical experience with a new IA detection DLA.

Methods A DLA was developed at Site 1 to predict the existence and locations of IAs >2 mm in 3D head CTA volumes. It localizes IAs using an improved 3D UNet to regress the bounding boxes of suspicious locations. IA presence is confirmed by a multi-resolution 3D DenseNet at each suspicious location. The model was trained on 436 studies and tested on 696 studies from site 1. To validate robustness against protocol variability, it was retrospectively tested on 337 volumes (149 positives, 188 negatives) from 4 additional sites with various types of scanners. A neuroradiologist/trained fellow from each site annotated bounding boxes around the IAs with 3DSlicer. The model's performance was assessed by comparing its predicted aneurysm locations to the annotated boxes.

Results The model achieved a lesion-level sensitivity of 0.72 (95% CI: 0.66 - 0.75) with 1.4 false positives per volume (FPPV, 95% CI: 1.22 - 1.57). Sensitivity ranged 0.84 (1.72 FPPV) - 0.67 (1.40 FPPV) amongst 5 sites. Performance variation was secondary to testing on images from scanners the model had not been trained on (unseen). Removing unseen scanners, the model achieved sensitivity of 0.77 (95% CI: 0.68 - 0.84) with 1.51 FPPV (95% CI: 1.24 - 1.82). Patient-level area under curves (AUCs) on the external sites were comparable to that of site 1 dataset, which was 0.88 (95% CI: 0.84 - 0.92). The model performed better in the detection of internal carotid and anterior communicating artery IAs > 3 mm.

Conclusions This DLA for IA detection showed robust performance in detecting IAs > 3 mm. DLAs may reliably help

Abstract E-107 Table 1 Stratified performance of the model on the external datasets using the parameters set for Site 1

Subset (No. of volumes)	Lesion-level Sensitivity [95% CI]	False Positive per Volume (FPPV) [95% CI]
Site 2 (40)	0.77 [0.56, 1.00]	0.91 [0.54, 1.38]
Site 3 (57)	0.84 [0.70, 0.95]	1.72 [1.29, 2.16]
Site 4 (149)	0.67 [0.56, 0.77]	1.40 [1.13, 1.65]
Site 5 (91)	0.72 [0.60, 0.82]	1.41 [1.08, 1.84]
GE (89)	0.75 [0.63, 0.86]	1.40 [1.08, 1.77]
Siemens (78)	0.83 [0.68, 0.95]	1.70 [1.34, 2.18]
Philips, unseen (83)	0.73 [0.61, 0.84]	1.50 [1.12, 1.97]
Toshiba/Canon, unseen (87)	0.62 [0.37, 0.77]	1.16 [0.86, 1.53]

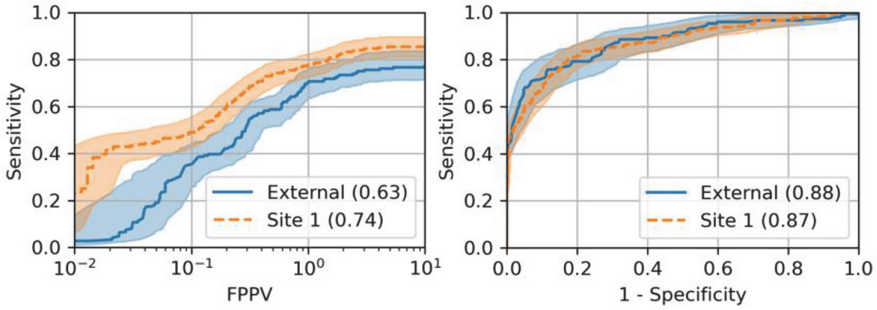

Figure. The free-response receiver operation characteristics (FROC) curve (left) and the ROC curve (right) of the model on the external (Site 2 - 5) and Site 1 datasets. The numbers in the FROC legends gave the average sensitivity at 0.125, 0.25, 0.5, 1, 2, 4, 8 FPPV. The numbers in the ROC legends gave the area under the curve (AUC).

Abstract E-107 Figure 1 The free-response receiver operation characteristics (FROC) curve (left) and the ROC curve (right) of the model on the external (Site 2 – 5) and Site 1 datasets. The numbers in the FROC legends gave the average sensitivity at 0.125, 0.25, 0.5, 1, 2, 4, 8 FPPV. The numbers in the ROC legends gave the area under the curve (AUC)

detection of IAs on CTA, particularly in the community practices less familiar with intracranial vascular imaging. Different scanners can lead to performance variability. This can be avoided by training with data from different scanners.

Disclosures D. Wu: 1; C; National Institute of Health. **E. Orru':** None. **S. Ferraciolli:** None. **A. Ashok:** 1; C; NIHR Academic Clinical Fellowship. **A. Sorby-Adams:** None. **M. Guindy:** None. **D. Montes:** None. **A. Medina:** None. **G. Bianco:** None. **J. Kaggie:** 1; C; NIHR Cambridge BRC. **D. Rabina:** None. **O. Ashush:** None. **X. Han:** None. **Y. Baror:** None. **M. Patel:** 4; C; Rhino HealthTech Inc. **I. Dayan:** 4; C; Rhino HealthTech Inc.. **J. Romero:** None. **R. González:** 1; C; National Institute of Health. 2; C; MR Access, Inc.. 4; C; MR Access, Inc.. **C. Wald:** None. **F. Kitamura:** 2; C; MD.ai, GE Healthcare. **P. Kuriki:** None. **T. Matys:** 1; C; NIHR Cambridge BRC. 2; C; NHS. **Q. Li:** 1; C; National Institute of Health.

E-108 RUPTURED INTRACRANIAL ANEURYSM PRESENTING AS ISOLATED ACUTE SUBDURAL HEMORRHAGE

[1]D Babici, [1]P Johansen, [1]SL Newman, [2]E Packer, [2]B Snelling. *[1]Neurology, Florida Atlantic University, Boca Raton, FL; [2]Neurological Surgery, Boca Raton Regional Hospital, Boca Raton, FL*

10.1136/neurintsurg-2022-SNIS.219

Introduction Ruptured intracranial aneurysms are often associated with serious neurologic sequelae, often as a result of subarachnoid or intraparenchymal hemorrhage. Less commonly, ruptured intracranial aneurysms can lead to subdural hemorrhage. However, the characteristic clinical presentation and optimal treatment of associated subdural hemorrhage are unclear due to the paucity of such cases that exist in the current literature. Affected patients may complain of nonspecific symptoms such as headaches, nausea, and confusion. Because of the severity of the disease, rapid diagnosis and intervention is required to lower the high morbidity and mortality rates. Commonly used treatment options include endovascular coiling and microsurgical clipping. Neuroendovascular surgery is often preferred, especially in aneurysms not amenable to surgical clipping, in poor surgical candidates, and in cases with endovascularly favorable anatomy.

Methods Single case study.

Case Description A 65-year-old female with no known past medical history suddenly developed right-sided weakness and leftward gaze deviation, prompting a stroke alert to be initiated prior to arrival in the ED. Once arrived at the hospital, she became drowsy and unable to follow commands. After several vomiting episodes, she was emergently intubated for airway protection. Her initial blood pressure was 240/120, for which labetalol and nicardipine were administered. CT scan of the head revealed a left-sided subdural hematoma with a left-to-right midline shift and scant subarachnoid hemorrhage in the Sylvan fissure. Given the patient's declining neurological exam and radiographic findings, she was taken to the operating room for emergent evacuation of the subdural hematoma. Following surgery, MRA of the brain was ordered and revealed a left-sided 6mm posterior communicating artery aneurysm. Urgent coil embolization of the aneurysm was successfully performed via right radial artery access with Raymond-Roy class 2 occlusion. In the following days, the patient's right-sided weakness significantly improved, and her sensory examination remained unremarkable with intact deep tendon reflexes.

Conclusion In rare cases, ruptured intracranial aneurysms can be associated with isolated subdural hemorrhage. Common treatment options include endovascular coiling and microsurgical clipping. However, endovascular repair is often preferred especially when the patient may not be able to tolerate a surgical procedure, as was the case with this patient. In this case, the patient presented with stroke-like symptoms and was found to have a subdural hemorrhage. After emergent craniotomy to evacuate the hematoma, successful endovascular coiling was performed, and the patient was stabilized for further management>

Disclosures D. Babici: None. **P. Johansen:** None. **S. L. Newman:** None. **E. Packer:** None. **B. Snelling:** None.